3D-mixed-mode-loading: material characteristic values and criteria's validity

H. A. Richard, A. Eberlein
University of Paderborn, Institute of Applied Mechanics, Pohlweg 47-49, 33098 Paderborn, Germany
richard@fam.upb.de, http://mb.uni-paderborn.de/fam/
eberlein@fam.upb.de, http://mb.uni-paderborn.de/fam/

ABSTRACT. In many structures and components cracks, which are exposed to a 3D-mixed-mode-loading, occur due to multiaxial loading situation. A reliable evaluation of those components requires fracture mechanical criteria validated by experimental investigations. Within this article 3D-mixed-mode criteria for static as well as cyclic loadings will be presented. Experiments for pure mode I-loading, pure mode II-loading, pure mode III-loading and 2D- as well as 3D-mixed-mode-loading combinations are performed using specially developed specimens and loading devices. By comparing the experimental results with criteria a widely validity of criteria and a generally conservative behaviour are revealed.

KEYWORDS. 3D-mixed-mode Criteria; Threshold Values; Fracture Toughness; CTSR-specimen.

INTRODUCTION

In many practical cases crack growth leads to fatigue fracture or abrupt failure of components and structures. For reasons of a reliable quantification of the endangerment due to sudden fracture of a component it is of huge importance to know the limiting values (fracture toughness) for the beginning of instable crack growth as well as the threshold values for the fatigue crack growth. This contribution deals with the complex problem of crack growth under mixed-mode-loading. It will present a comparison between concepts, which characterises the superposition of mode I and mode II (2D-mixed-mode) as well as the superposition of all three modes (mode I, mode II and mode III) for spatial loading conditions, and experimental results for stable and unstable crack growth.

MULTIAXIAL STRESS FIELD AND FRACTURE MODES

In linear-elastic fracture mechanics the characterisation of the loading situation at the crack front and in its neighbourhood is based on stresses and displacements. Generally, a crack can be loaded by a multiaxial stress field consisting of six stress components. As Fig. 1 exemplary shows on a boarder crack with the length a in a volume cube, different stresses causes various crack loadings (fracture modes). σ_y induces a crack opening (mode I). A mode I-loaded crack grows perpendicular to the normal stress σ_y. Due to the shear stress τ_{xy} the crack kinks out of its previous direction in shear stress plane. In this case a mode II-loading on crack is present. The shear stress τ_{yz} effects an anti-plane shear loading (mode III) at the crack, which leads to a crack twisting. Furthermore the initial crack separates in multiple daughter crack segments.

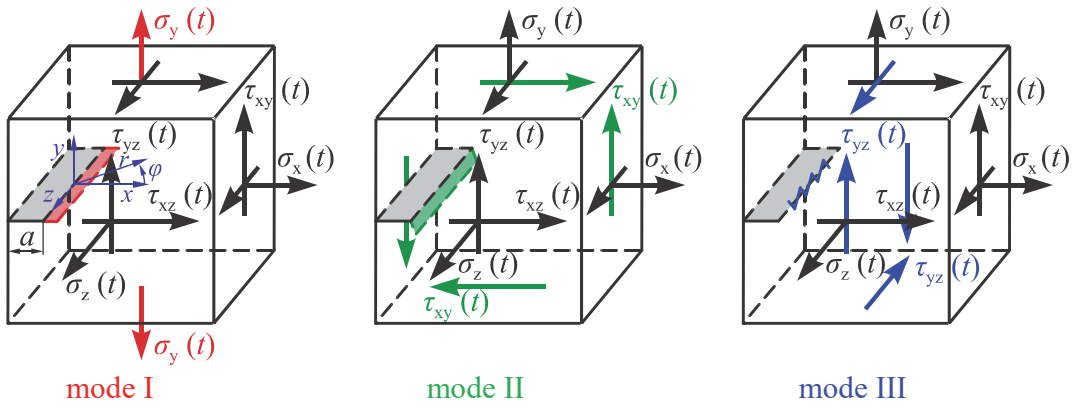

Figure 1: Stress components and fracture modes

Nevertheless, cracks in real structures often experience complex loading conditions, which are to a superposition of the three basic fracture modes. For plane crack problems in the case of 2D-mixed-mode the stress distribution can be described with the help of the near field solution and the polar coordinates r and φ (see Fig. 1) by the following equation as [1]:

$$\sigma_{ij}(r,\varphi)=\frac{1}{\sqrt{2\pi\cdot r}}\cdot\left[K_I\cdot f_{ij}^{I}(\varphi)+K_{II}\cdot f_{ij}^{II}(\varphi)\right] \tag{1}$$

with $i,j = x,y$.
The calculation of the stress distribution spatially crack problems loaded under 3D-mixed-mode is completed by a third term to:

$$\sigma_{ij}(r,\varphi)=\frac{1}{\sqrt{2\pi\cdot r}}\cdot\left[K_I\cdot f_{ij}^{I}(\varphi)+K_{II}\cdot f_{ij}^{II}(\varphi)+K_{III}\cdot f_{ij}^{III}(\varphi)\right] \tag{2}$$

with $i,j = x,y,z$.
K_I, K_{II} and K_{III} are from Irwin established stress intensity factors. They are assigned to the basic fracture modes of a crack and defined by Eq. 3. The stress intensity factor depends on the stress (σ_y, τ_{xy} or τ_{yz}), the crack length a and on the boundary correction factor (Y_I, Y_{II} or Y_{III}). If the loading of a structure creates a non-symmetrical, singular stress field in the vicinity of the crack front, then the crack front deforms in a way that not only an opening, but also a planar and non-planar displacement of the two crack flanks can be found. Consequently, the stress field in the vicinity of the crack is superimposed by all of three stress intensity factors K_I, K_{II} and K_{III}.

$$\begin{aligned} K_I &= \sigma_y\cdot\sqrt{\pi\cdot a}\cdot Y_I \\ K_{II} &= \tau_{xy}\cdot\sqrt{\pi\cdot a}\cdot Y_{II} \\ K_{III} &= \tau_{yz}\cdot\sqrt{\pi\cdot a}\cdot Y_{III} \end{aligned} \tag{3}$$

Unstable Crack Growth under 2D- und 3D-Mixed-Mode-loading

Of enormous interest concerning the part dimensioning is the beginning of unstable crack growth, because the consequence often is a high material and immaterial damage. To predict unstable crack growth under 2D- and 3D-mixed-mode-loading many criteria exist, which compare the occurred stress or stress intensity factor with a critical stress σ_C or the fracture toughness K_{IC}. Some of them are listed below.

3D-criterion by Richard

The beginning of unstable crack growth as well as the crack growth direction e.g. can be determined by using the following fracture criteria:

- Criterion by Erdogan and Sih [2]
- 2D-criterion by Richard [3, 4]
- Criterion by Schöllmann et al. [1, 5, 6]
- 3D-criterion by Richard [4, 7].

Within this contribution only the 3D-criterion by Richard is described explicitly. This criterion is developed in order to simplify the prediction of crack growth under multiaxial loading. Due to the fact that engineers often use the classical stress hypotheses the formula is helpful for practical application. Unstable crack growth will occur, if the local loading condition along the crack front reaches the fracture toughness value. This situation can be described by the following fracture criterion [4]:

$$K_V = \frac{K_I}{2} + \frac{1}{2}\cdot\sqrt{K_I^2 + 4\cdot(\alpha_1\cdot K_{II})^2 + 4\cdot(\alpha_2\cdot K_{III})^2} = K_{IC} \tag{4}$$

where $a_1 = K_{IC}/K_{IIC}$ and $a_2 = K_{IC}/K_{IIIC}$. For the material parameters $a_1 = 1.155$ and $a_2 = 1.0$ Eq. 4 is in excellent agreement with the K_V-prediction of the criterion by Schöllmann et al.

Experimental Investigations for unstable crack growth under mixed-mode-loading conditions

In the following, experimental investigations on 2D- and 3D-mixed-mode loadings are presented. In the past several specimen types for 2D-mixed-mode problems have been proposed [3, 7, 8]. Among others, the CTS-specimen together with its loading device [9, 10] has proven its applicability. Therefore only the CTS-specimen will be discussed in the following. The loading device in Fig. 2 allows applying pure mode I-, pure mode II- as well as almost every 2D-mixed-mode-loading combination to the CTS-specimen by using just a uniaxial tension testing machine. For the purpose of varying the mixed-mode-loading only the loading angle α has to be changed.

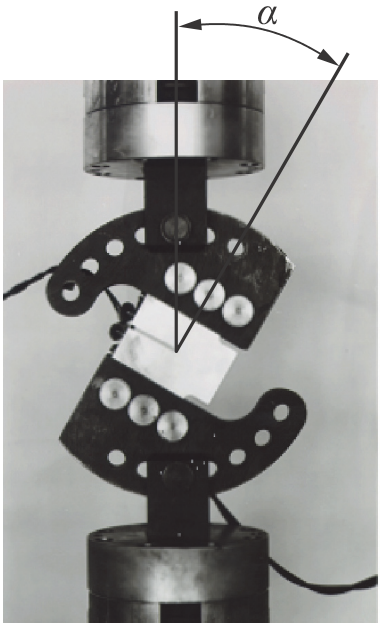

Figure 2: Loading device for plane mixed-mode I + II-loading

Referring to the AFM-specimen [11] a new specimen, so-called CTSR-specimen, with the corresponding loading device, shown in Fig. 3, has been developed [12] for investigating 3D-mixed-mode-loadings. This new specimen and corresponding loading device enables any combination of mixed-mode-loading including pure mode I-, pure mode II- and pure mode III-loading. The loading device allows to generate any ratio of mode I to mode II/mode III by changing the loading angle a in 15°-steps. By rotating the so-called turret also in 15°-steps (varying the second loading angle β) inside

the loading device the ratio of mode II or mode III load is set. Both loading angles a and β can be adjusted in the range from 0° to 90°, whereby the load line of action always passes through the centre of specimen. The detailed CTSR-specimen geometry with relevant dimensions is illustrated in [13, 18]. This paper will focus on eperimental results investigated by CTSR-specimen and the corresponding loading device.

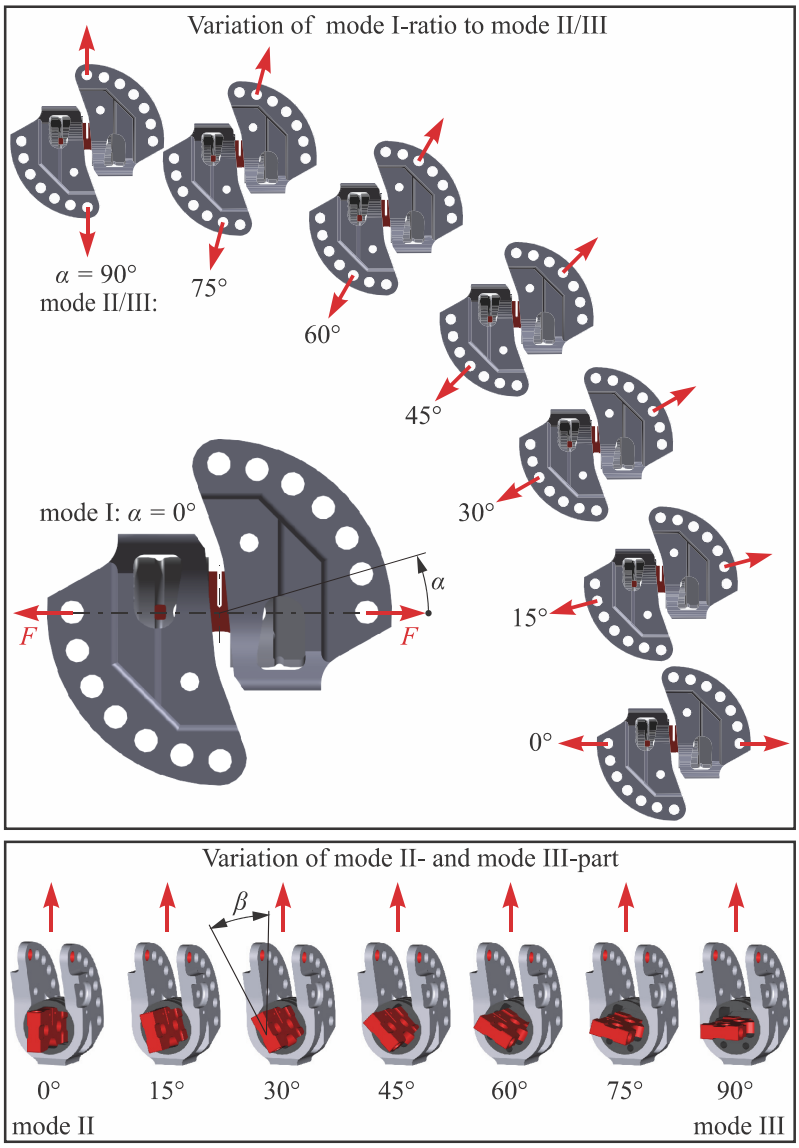

Figure 3: Loading device for 3D-mixed-mode-loading

Comparison of experimental results with fracture criteria

In the following results of fracture experiments and comparison with 3D-criterion by Richard are shown and discussed. The points in Fig. 4 are the fracture toughness values for PMMA, measured on CTSR-specimens. By comparison with the 3D-criterion by Richard or the criterion by Schöllmann et al., mentioned in this paper, a significant variation of the fracture toughness values determined by mode III-loading is noticeable.

The resulting fracture toughness values for pure mode III-loading K_{IIIC} are around factor 2.7 above the hypothesis [14]. Furthermore, it is visible that the less the mode III ratio the better the congruence with the predictions of the hypothesis. As soon as there is no mode III-loading the measured values are very close to the criterion by Richard. The reason for the big spread between the hypothesis and the mode III fracture toughness values is possibly the building of a new fragmented crack front with many facets, which is not considered in the criteria yet.

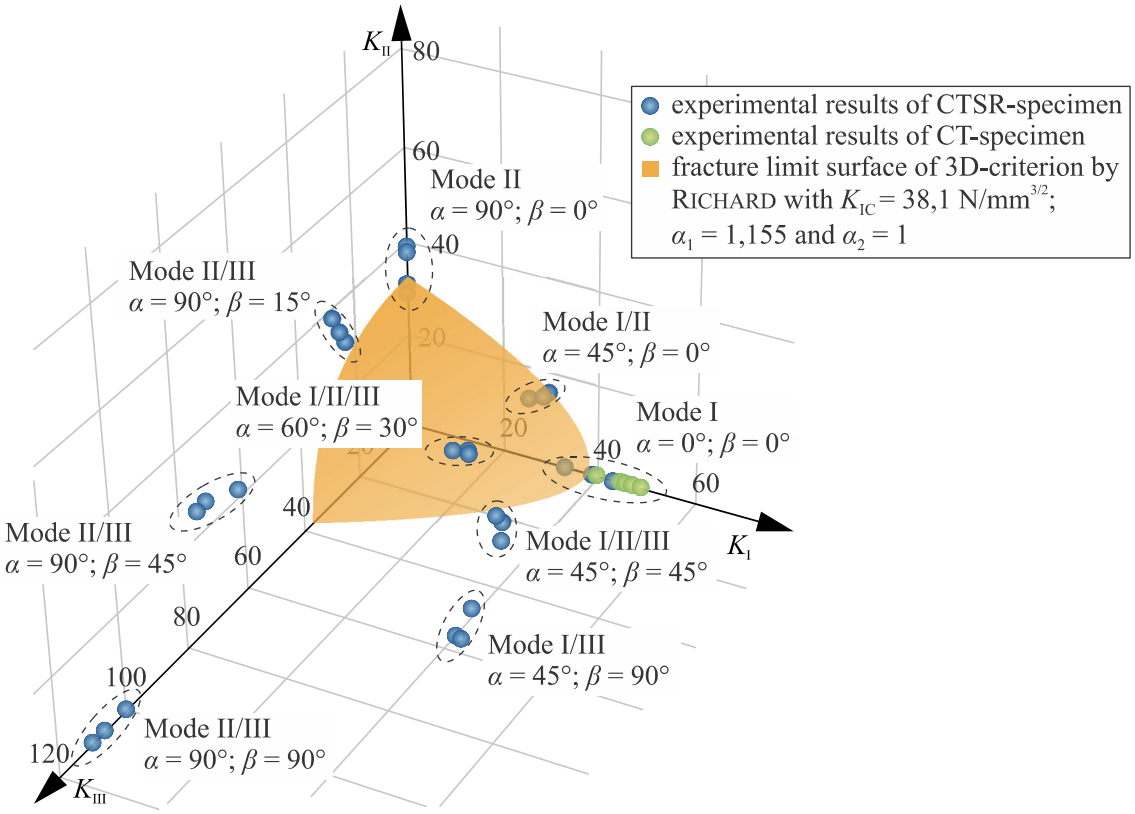

Figure 4: Experimental results for PMMA in contrast to the criterion by Richard

FATIGUE CRACK GROWTH UNDER 2D- AND 3D-MIXED-MODE-LOADING

Among the experimental determination of the fracture limit surface presented in Fig. 4 for PMMA the investigation of the threshold value surface of different materials under 2D- and 3D-mixed-mode-conditions is important too, to characterise the crack growth behaviour under combined loading situations.

Cyclic comparative stress intensity factor for fatigue crack growth

A crack, which is subjected to an arbitrary mixed-mode-loading, is able to propagate under fatigue crack growth conditions, if the local crack front loading combined of mode I, mode II and mode III portions is located in between the threshold value and a critical cyclic stress intensity factor. This condition can be written down by the formula:

$$\Delta K_{I,th} < \Delta K_V < \Delta K_{IC} \tag{5}$$

Hereby ΔK_V is the cyclic comparative stress intensity factor, which can be derived from Eq. 4 using as before $a_1 = 1.155$ and $a_2 = 1.0$:

$$\Delta K_V = \frac{\Delta K_I}{2} + \frac{1}{2} \cdot \sqrt{\Delta K_I^2 + 5{,}336 \cdot \Delta K_{II}^2 + 4 \cdot \Delta K_{III}^2} \tag{6}$$

Experimental determinations of threshold values under combined loading

The mixed-mode threshold values were determined using the load rising amplitude test [15, 16, 17]. Before the fatigue test the specimen were pre-cracked under cyclic compression. The advantage of pre-cracking the specimen in cyclic compression are, however, the left residual tensile stresses, which may cause cyclic plastic deformation and crack initiation [15]. The threshold tests were performed at a constant load ratio of $R = 0.1$ by increasing the load amplitude in

steps until the threshold value is reached. A more detailed information to the experimental procedure and chosen parameters can be found in [18].

Comparison of experimental results with fatigue criterion

The mixed-mode threshold values determined by the procedure described above are illustrated in Fig. 5. The threshold values of Al7075-T651 measured by Schirmeisen [13] in comparison of the criterion by Richard show for pure mode I-loading, 2D-mixed-mode-loading and for mixed-mode II + III-loading with small mode III-ratio a good congruence with the threshold value surface of the criterion by Richard. A significant variation, with around a factor of 2.2 above the hypothesis [14], depict the threshold values for pure mode III-loading. The threshold values measured by Eberlein [18] in total are closer to the threshold value surface of the hypothesis. The variation in average is around factor 1.8 above the hypothesis. In addition a comparison of other materials [19, 20] show partially similar threshold value ratios $\Delta K_{II,th}/\Delta K_{I,th}$ and $\Delta K_{III,th}/\Delta K_{I,th}$ (see threshold values for austenitic steel in Fig.5). Ferritic steel exhibits completely other threshold value ratios. Nevertheless, the determined mixed-mode threshold values for different materials in comparison with the criterion by Richard point out that this criterion possesses a widely validity and a generally conservative behaviour.

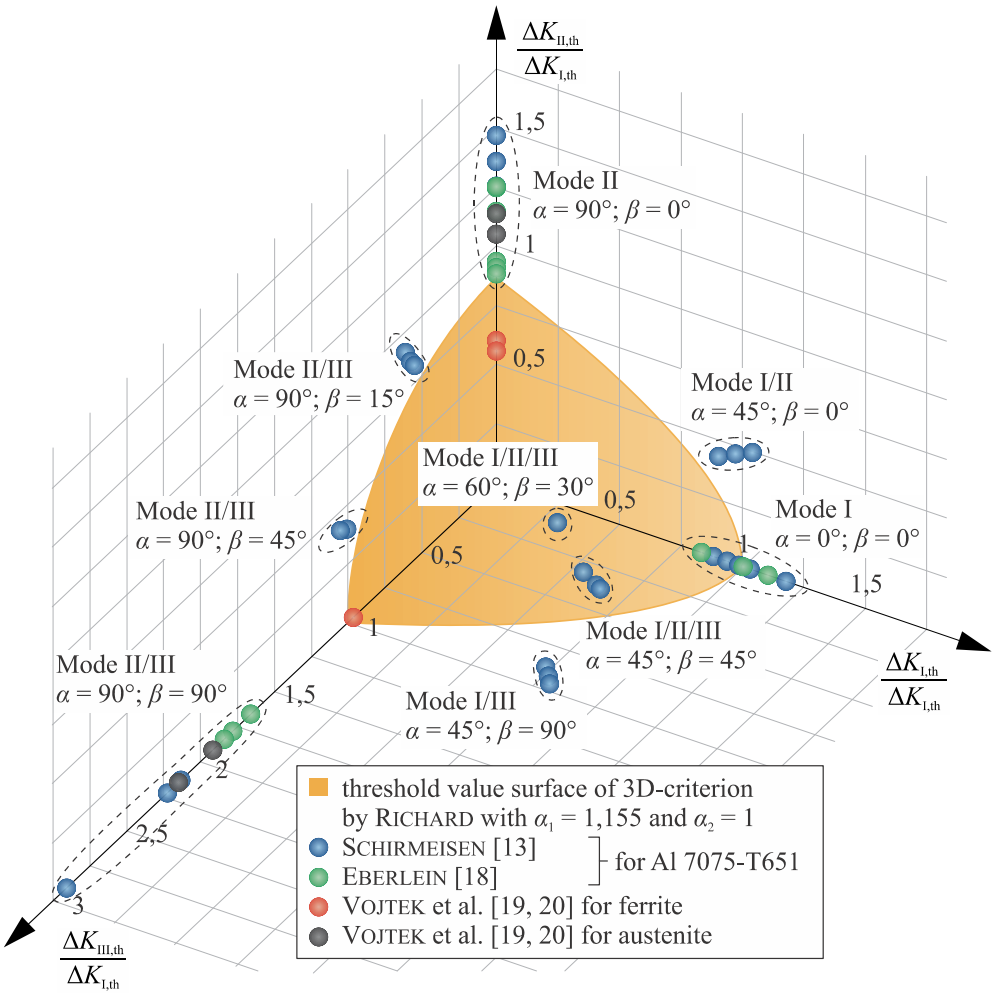

Figure 5: Mixed-mode threshold values in contrast to criterion by Richard

REFERENCES

[1] Richard, H.A.., Sander, M., Fulland, M., Theoretical crack path prediction, FFEMS, 28 (2005) 3–12.
[2] Erdogan, F., Sih, G.C., On the crack extension in plates under plane loading and transverse shear, J. Basic Eng., 85 (1963) 519-525.

[3] Richard, H.A., Bruchvorhersage bei überlagerter Normal- und Schubbeanspruchung von Rissen, VDI-Verlag, Düsseldorf, (1985).
[4] Richard, H.A., Safety estimation for construction units with cracks under complex loading. Int. J. Mater. Product. Technol., 3 (1988) 326-338.
[5] Schöllmann, M., Richard, H.A., Kullmer, G., Fulland, M., A new criterion for the prediction of crack development in multiaxially loaded structures. Int. J. Frac., 117 (2002) 129-141.
[6] Schöllmann, M., Kullmer, G., Fulland, M., Richard, H.A., A new criterion for 3D crack growth under mixed-mode (I + II + III) loading. in: M.M. de Freitas (Ed.), Proceedings of the 6th International Conference on Biaxial/Multiaxial Fatigue & Fracture, Volume 2, Lisboa, Portugal, (2001) 589-596.
[7] Richard, H.A., Schöllmann, M., Fulland, M., Sander, M., Experimental and numerical simulation of mixed mode crack growth, in: M.M. de Freitas (Ed.), Proceedings of the 6th International Conference on Biaxial/Multiaxial Fatigue & Fracture, Lisboa, Portugal, 2 (2001) 623-630.
[8] Richard, H.A., in: M.W. Brown, K.J. Miller (Eds.), Biaxial and Multiaxial Fatigue, Mechanical Engineering Publications, London, (1989) 217-229.
[9] Richard, H.A., Benitz, K., A loading device for the creation of mixed mode in fracture mechanics, Int. J. Frac., 22 (1983) R55-58.
[10] Richard, H.A., in: S.R. Valluri et al. (Eds.), Advances in Fracture Research, Pergamon Press, Oxford, (1984) 3337-3344.
[11] Richard, H.A., Praxisgerechte Simulation des Werkstoff- und Bauteilverhaltens durch überlagerte Zug-, ebene Schub- und nichtebene Schubbelastung von Proben, VDI-Verlag, Düsseldorf, (1983) 269-274.
[12] Schirmeisen, N.-H., Richard, H.A., Weiterentwicklung der AFM-Probe zur experimentellen Analyse räumlicher Mixed-Mode-Beanspruchung von Rissen, DVM-Bericht 241, Bruchmechanische Werkstoff- und Bauteilbewertung: Beanspruchungsanalyse, Prüfmethoden und Anwendungen, Deutscher Verband für Materialforschung und –prüfung e.V. Berlin (2009) 211-220.
[13] Schirmeisen, N.-H., Risswachstum unter 3D-Mixed-Mode-Beanspruchung, VDI-Verlag, Düsseldorf, (2012).
[14] Richard, H.A., Schirmeisen, N.-H., Eberlein, A., Experimental investigations on mixed-mode-loaded cracks, Proceedings of the 4th International Conference on Crack Paths, CD-Rom, Gaeta, Italy, (2012).
[15] Tabernig, B., Pippan, R., Determination of the length dependence of the threshold for fatigue crack propagation, Engng. Frac. Mech., 69 (2002) 899-907.
[16] Campbell, J.P., Ritchie, R.O., Mixed-Mode, high-cycle fatigue-crack growth thresholds in Ti-6Al-4V: I. A comparison of large- and short-crack behavior, Engng. Frac. Mech., 67 (2000) 209-227.
[17] Nalla, R.K., Campbell, J.P., Ritchie, R.O., Mixed-Mode, high-cycle fatigue-crack growth thresholds in Ti-6Al-4V: Role of small cracks, Int. J. Fat., 24 (2002) 1047-1067.
[18] Eberlein, A., Einfluss von Mixed-Mode-Beanspruchung auf das Ermüdungsrisswachstum in Bauteilen und Strukturen. VDI-Verlag, Düsseldorf, (2016).
[19] Vojtek, T., Pokluda, J., Paths of shear-mode Cracks in Ferritic and Austenitic Steel. Proceedings of the 4th International Conference on Crack Paths, CD-Rom, Gaeta, Italy, (2012).
[20] Vojtek, T., Pippan, R., Hohenwarter, A., Holán, L., Pokluda, J., Near-threshold propagation of mode II and mode III fatigue cracks in ferrite and austenite, Act. Mater., 61 (2013) 4625-4635.